Open Access Library Journal
2024, Volume 11, e12430
ISSN Online: 2333-9721
ISSN Print: 2333-9705

Analytical Approximation to the Bound State Energies and Wave Functions of the Schrödinger Equation with the Gaussian Potential Well in One Dimension

Hippolyte Nyengeri[1], Rénovat Nizigiyimana[1], Rubin Ndikumana[2]

[1]Département de Physique, Faculté des Sciences, Université du Burundi, Bujumbura, Burundi
[2]Lycée Comunal de Buruhukiro, Rumonge, Burundi
Email: hippolyte.nyengeri@ub.edu.bi

How to cite this paper: Nyengeri, H., Nizigiyimana, R. and Ndikumana, R. (2024) Analytical Approximation to the Bound State Energies and Wave Functions of the Schrödinger Equation with the Gaussian Potential Well in One Dimension. *Open Access Library Journal*, **11**: e12430.
https://doi.org/10.4236/oalib.1112430

Received: October 4, 2024
Accepted: November 23, 2024
Published: November 26, 2024

Abstract

In this paper, an efficient approximate analytical technique for solving the one-dimensional Schrödinger equation (SE) with an attractive Gaussian potential is developed. This technique is based on approximating the Gaussian potential well (GPW) with the modified Pöschl-Teller potential (MPTP), and on the first- and second-order perturbation treatment of the resulting bound state energies and wave functions. In order to illustrate the excellent performance of our technique, we compare our results with those obtained from the exact Hamiltonian diagonalization on a finite-real basis of associated Legendre functions (ALF).

Subject Areas

Quantum Mechanics

Keywords

Schrödinger Equation, Bound States, Gaussian Potential Well, Modified Pöschl-Teller Potential, Time-Independent Perturbation Theory

1. Introduction

The modified Pöschl-Teller potential (MPTP) and the Gaussian Potential Well (GPW) are among the potentials which are frequently discussed in the literature [1]-[10] as examples of potentials that have bound states. Exact analytical solutions of the time-independent Schrödinger equation (TISE) with the MPTP can

be found in many written sources [1]-[3] [5].

The main purpose of this work is to develop an approximate analytical technique for bound state energies and wave functions of the one-dimensional TISE with the GPW of the form

$$V(x) = -V_0 \exp\left(-x^2/2\sigma^2\right) \tag{1}$$

where $V_0 > 0$ and $\sigma > 0$. To achieve this goal, we follow these steps:

Step 1. Model the GPW (1) with the MPTP in the TISE.

Step 2. Solve the resulting TISE to find exact eigenvalues and normalized eigenfunctions for all the bound states.

Step 3. Model the difference between the potential $V(x)$ and its approximation with the so-called Pöschl-Teller Polynomial Potential (PTPP) [11], and then use the time-independent perturbation Theory (TIPT) [12] to compute the first- and second-order corrections to the energy levels and wave functions obtained in step 2.

The rest of this paper is organized as follows. In section 2, we consider the exactly solvable SE obtained by approximating the GPW by a MPTP, and give analytical expressions of the bound state energies and normalized wave functions of this equation. We also calculate the first- and second-order corrections to these energies and wave functions with the aid of the TIPT. In order to facilitate these calculations, we use the PTPP to model the perturbing Hamiltonian, *i.e.*, the difference between the GPW and its approximation in terms of the MPTP. In section 3, we present and comment results for two special cases, *i.e.*, the case of $(V_0, \sigma) = (4.5 \text{ a.u.}, 2.65 \text{ a.u.})$ and the case of $(V_0, \sigma) = \left(0.63 \text{ a.u.}, 2.65/\sqrt{2} \text{ a.u.}\right)$ which is very interesting since the lowest two eigenvalues associated with it are -0.4451 and -0.1400 a.u., that correspond closely to the lowest two energy levels of the xenon atom [13]. In each case, the bound state energies and wave functions obtained by means of our method are compared with those given by the exact Hamiltonian diagonalization on a finite-real basis of associated Legendre functions (ALF). The conclusion is given in section 4.

2. Materials and Methods

2.1. Reference and Perturbing Hamiltonians

The SE of a particle with mass m and potential $V(x)$ given by Equation (1) can be written as

$$\left[-\frac{\hbar^2}{2m}\frac{\mathrm{d}^2}{\mathrm{d}x^2} - V_0 \exp\left(-x^2/2\sigma^2\right)\right]\psi(x) = E\psi(x) \tag{2}$$

Here, $\psi(x)$ is the wave function and E is the energy eigenvalue.

We have to indicate that by an estimation based on the WKB method, the number of bound states supported by the potential of interest is approximated by [7] [14] [15]

$$nbst = \left\lfloor 4\sigma\sqrt{V_0/2\pi} + 1/2 \right\rfloor \tag{3}$$

where $\lfloor\ \rfloor$ represents the floor function, which for positive numbers is simply the integer part. But so far, to the best of our knowledge, exact analytical forms of the bound state energies and wave functions of this potential have not been reported. Therefore, it is of considerable interest to find a good analytical approximation for the solution of the SE (2). To achieve this, we appeal to a perturbation procedure which yields approximate eigenfunctions as well as eigenvalues of the SE under consideration. The perturbation approach we consider here is based on approximating the GPW with a MPTP, i.e.,

$$-V_0 \exp\left(-x^2/2\sigma^2\right) \approx -V_0 \operatorname{sech}^2\left(\tilde{\alpha}x/\sqrt{2}\sigma\right) \tag{4}$$

which suggests us to choose as reference or unperturbed Hamiltonian the operator H_0 given by

$$H_0 = -\frac{\hbar^2}{2m}\frac{\mathrm{d}^2}{\mathrm{d}x^2} - V_0 \operatorname{sech}^2\left(\tilde{\alpha}x/\sqrt{2}\sigma\right) \tag{5}$$

and as perturbing Hamiltonian H_1 the difference between the GPW and its approximation in terms of the MPTP:

$$H_1 = -V_0\left[\exp\left(-x^2/2\sigma^2\right) - \operatorname{sech}^2\left(\tilde{\alpha}x/\sqrt{2}\sigma\right)\right]. \tag{6}$$

It is worth noting that the symbol $\tilde{\alpha}$ that appeals in Equations (4), (5) and (6) is an adjustable parameter. To determine this parameter, we consider the independent variable $\xi \in]-\infty,+\infty[$. We then discretize this variable in the interval $[0,20]$ and evaluate the function $f_G(\xi) \equiv -\exp\left(-\xi^2\right)$ at $X_k = kh$ (for $k = 1,2,\cdots,p-1$ where p is the number of mesh points and h the step size), thus creating two p-vectors X and Y such that $X_k = kh$ and $Y_k = -\exp\left(-X_k^2\right)$. Thereafter we appeal to the maple 18 software (the Fit command) to construct the function $-\operatorname{sech}^2\left(\tilde{\alpha}\xi\right)$ that best fits the above set of data points, i.e., $\left(X_k, Y_k\right)$, $k = 0,1,2,\cdots,p-1$. It is worth noting that in maple, the Fit command fits a model function to given data by minimizing the least-square error. In the case we are concerned with, the calling sequence is: $Fit\left(-\operatorname{sech}\left(\tilde{\alpha}\xi\right)^2, X, Y, \xi\right)$. With the number of digits equals 14, we found

$$\tilde{\alpha} = 1.1045570178649. \tag{7}$$

Figure 1 (resp. Figure 2) shows the graph of the GPW, that of its approximation in terms of the MPTP and that of the error in this approximation when $V_0 = 4.5$ a.u. (resp. $V_0 = 0.63$ a.u.) and $\sigma = 2.65$ a.u. (resp. $\sigma = 2.65/\sqrt{2}$ a.u.). These figures show that the GPW is in close agreement with the MPTP.

Moreover, in Figure 3, we plot the perturbing Hamiltonian H_1 as a function of the coordinate x for $V_0 = 1$ a.u. and various values of the parameter σ. This figure shows that when σ increases, $H_1(x)$ extends in the space, while its amplitude remains constant, which means that the MPTP is in close agreement with the GPW for a larger range of x at small values of σ. It can be verified that $y_{0m} \le H_1(x) \le y_{0p}$ where $y_{0m} = -0.03449339755585779$ and $y_{0p} = 0.03375328424820693$. Consequently, the amplitude of $H_1(x)$ equals $\left|y_{0m}\right|$ when $V_0 = 1$.

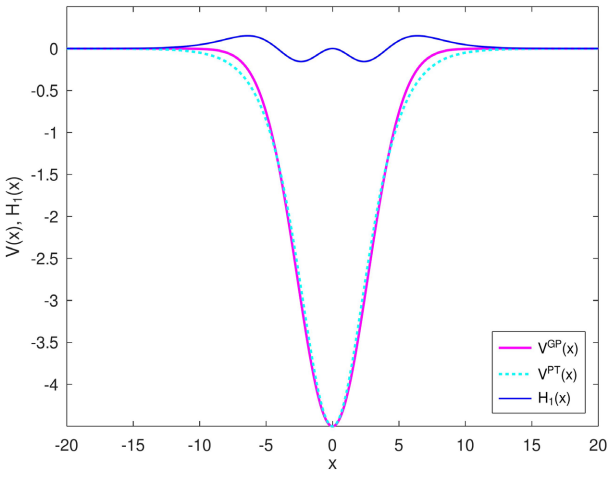

Figure 1. Plot of the GPW, its approximation in terms of the MPTP and the associated error when $V_0 = 4.5$ a.u. and $\sigma = 2.65$ a.u.

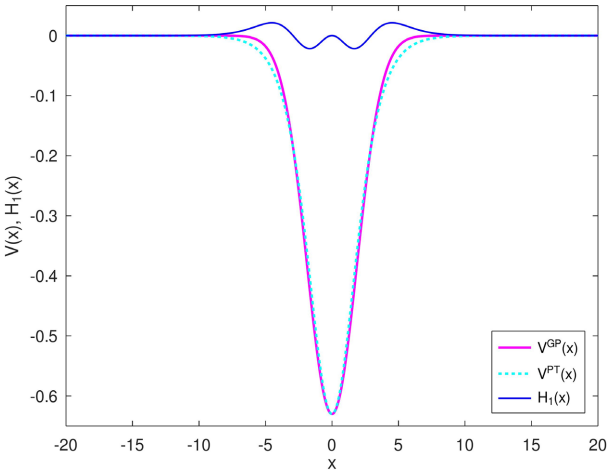

Figure 2. Plot of the GPW, its approximation in terms of the MPTP and the associated error when $V_0 = 0.63$ a.u. and $\sigma = 2.65/\sqrt{2}$ a.u.

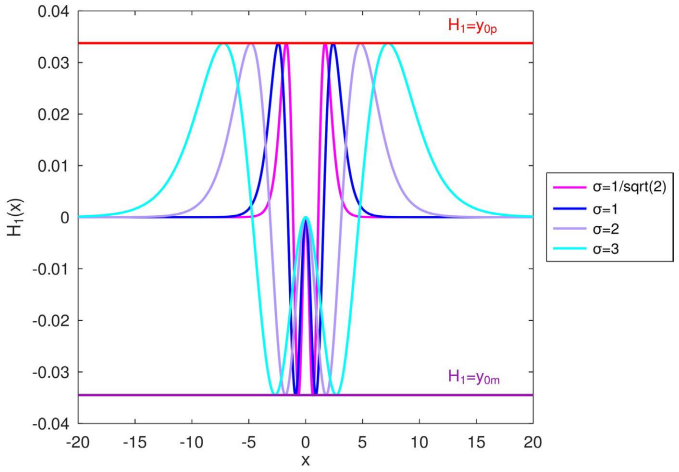

Figure 3. Perturbing Hamiltonian against the spatial coordinate x for a fixed value of $V_0 = 1$ a.u. and four different values of σ.

Because $H_1(x)$ is directly proportional to the parameter V_0 (see Equation (6)), its amplitude increases with this parameter. Consequently, only the values of V_0, for which $\max_x |H_1(x)|$ is small, are acceptable in the framework of our approximation.

2.2. Solution of the Schrödinger Equation Associated with the Reference Hamiltonian

The SE for the reference Hamiltonian H_0 can be written as

$$\left[-\frac{\hbar^2}{2m}\frac{\mathrm{d}^2}{\mathrm{d}x^2} - V_0 \operatorname{sech}^2(\alpha x)\right]\psi^{(0)}(x) = E^{(0)}\psi^{(0)}(x) \tag{8}$$

where

$$\alpha = \tilde{\alpha}/\sqrt{2}\sigma. \tag{9}$$

The spectrum of the Schrödinger operator H_0 has been studied in detail by several authors [1]-[3] [5] [16]. The bound state eigenvalues take the form

$$E_n^{(0)} = -\frac{\hbar^2\alpha^2}{2m}\left[\left(n+1/2-\sqrt{\nu+1/4}\right)^2\right], n = 0,1,\cdots, n < \sqrt{\upsilon+1/4}-1/2 \tag{10}$$

with

$$\upsilon = 2mV_0/\left(\hbar^2\alpha^2\right). \tag{11}$$

The corresponding eigenfunctions $\psi_n^{(0)}(x)$ can be written as

$$\psi_n^{(0)}(x) = N_n \operatorname{sech}^{\beta_n}(\alpha x)\, {}_2F_1\left(-n, a_n; c_n; u(x)\right) \tag{12}$$

where

$$a_n = \sqrt{4\upsilon+1} - n, \tag{13}$$

$$\beta_n = \sqrt{\upsilon+1/4} - 1/2 - n, \tag{14}$$

$$c_n = 1+\beta_n, \tag{15}$$

$$u(x) = \frac{1}{2}\left(1-\tanh(\alpha x)\right). \tag{16}$$

The normalization constants N_n are obtained from the equation

$$\int_{-\infty}^{+\infty}\left[\psi_n^{(0)}(x)\right]^2 \mathrm{d}x = 1 \tag{17}$$

and can be expressed as follows [16]:

$$N_n = \pm\left[\sum_{j=0}^{n}\frac{(-n)_j\left(1/2+\beta_n+\sqrt{4\nu+1}\right)_j}{(1+\beta_n)_j\, j!}\frac{4^{\beta_n}}{2\alpha}\frac{\Gamma(j+\beta_n)\Gamma(\beta_n)}{\Gamma(j+2\beta_n)}\right.$$
$$\left.\times\, {}_3F_2\left(-n, 1/2+\beta_n+\sqrt{4\nu+1}, j+\beta_n; 1+\beta_n, j+\beta_n; 1\right)\right]^{-1/2} \tag{18}$$

where $(a)_j$ is the Pochhammer symbol, *i.e.*,

$$(a)_j = a(a+1)\cdots(a+j-1) = \frac{\Gamma(a+j)}{\Gamma(a)},\ (a)_0 = 1. \tag{19}$$

2.3. Approximate Solution to the Eigenvalue Problem for the Perturbed Hamiltonian

According to the non-degenerate TIPT, the energy and wave function associated with the SE

$$(H_0 + H_1)|\psi_n\rangle = E_n|\psi_n\rangle \tag{20}$$

can be expanded as

$$E_n = E_n^{(0)} + E_n^{(1)} + E_n^{(2)} + \cdots, \tag{21}$$

$$|\psi_n\rangle = |\psi_n^{(0)}\rangle + |\psi_n^{(1)}\rangle + |\psi_n^{(2)}\rangle + \cdots \tag{22}$$

The parameters $E_n^{(k)}$ and the kets $|\psi_n^{(k)}\rangle$ represent the kth-order corrections to the eigen energies and eigenvectors respectively. The job of perturbation theory reduces then to the calculation of $|E_n^{(1)}\rangle$, $|E_n^{(2)}\rangle$, $\cdots$ and $|\psi_n^{(1)}\rangle$, $|\psi_n^{(2)}\rangle$, $\cdots$.

In our calculations, we shall be concerned only with the determination of $|E_n^{(1)}\rangle$, $|E_n^{(2)}\rangle$ and $|\psi_n^{(1)}\rangle$ with the aid of the following formulas [12] [14]:

$$|E_n^{(1)}\rangle = \langle\psi_n^{(0)}|H_1|\psi_n^{(0)}\rangle, \tag{23}$$

$$E_n^{(2)} = \sum_{k\neq n} \frac{\left|\langle\psi_n^{(0)}|H_1|\psi_k^{(0)}\rangle\right|^2}{E_n^{(0)} - E_k^{(0)}}, \tag{24}$$

$$|\psi_n^{(1)}\rangle = \sum_{k\neq n} \frac{\langle\psi_k^{(0)}|H_1|\psi_n^{(0)}\rangle}{E_n^{(0)} - E_k^{(0)}}|\psi_k^{(0)}\rangle. \tag{25}$$

Indeed, it is, in practice, very unlikely that terms of order higher than the second one is required.

Because of the parities of the perturbing Hamiltonian H_1 and the wave functions $\psi_n^{(0)}(x)$ (H_1 is even and $\psi_n^{(0)}(x)$ has same parity as n), it is necessary to calculate only the one-dimensional definite integrals (which appear in Equations (23), (24) and (25)) between states of the same parity. In order to facilitate this calculation, we model the Gaussian function $-\exp\left(-x^2/2\sigma^2\right)$ with a PTPP. More precisely, we write

$$-\exp\left(-x^2/2\sigma^2\right) \approx \sum_{i=1}^{K} B_i \operatorname{sech}^{2i}\left(\tilde{\alpha}x/\sqrt{2}\sigma\right) \tag{26}$$

where $\tilde{\alpha}$ is given by Equation (7); $B_1, B_2, \cdots, B_k$ are adjustable parameters, and K is a positive integer.

Choosing $K = 15$, and using the maple 18 Fit function, we find:

$$\begin{cases} B_1 = 0.04475365711493 \\ B_2 = -11.4548506185058 \\ B_3 = 45.772581796926 \\ B_4 = 177.799255220302 \\ B_5 = -3847.1826537244 \\ B_6 = 27513.46085554 \\ B_7 = -119694.9021684 \\ B_8 = 353986.505859662 \\ B_9 = -740228.775404985 \\ B_{10} = 1108311.085537 \\ B_{11} = -1182181.2620519 \\ B_{12} = 877597.630679932 \\ B_{13} = -431009.781694957 \\ B_{14} = 125902.352713473 \\ B_{15} = -16562.2934295893 \end{cases} \tag{27}$$

Combining Equations (26) and (6), we get

$$H_1 \approx V_0 \sum_{p=1}^{K} \tilde{B}_p \operatorname{sech}^{2p}\left(\tilde{\alpha} x / \sqrt{2}\sigma\right) \tag{28}$$

where

$$\tilde{B}_1 = B_1 + 1, \tag{29}$$

$$\tilde{B}_i = B_i,\ i = 2,3,\cdots,K. \tag{30}$$

In **Figure 4**, we plot the variation of $H_1(x)$ (Equation (6)) and that of its approximation H_1^{approx} given by

$$H_1^{approx}(x) = V_0 \sum_{p=1}^{15} \tilde{B}_p \operatorname{sech}^{2p}\left(\tilde{\alpha} x / \sqrt{2}\sigma\right) \tag{31}$$

with parameters $\tilde{B}_p, p = 1,2,\cdots,15$ given by Equations (27), (29) and (30). **Figure 5** shows the error in the approximation of $H_1(x)$, i.e.,

$$\Delta H_1(x) \equiv H_1(x) - H_1^{approx}(x) \tag{32}$$

It is obvious from **Figure 4** and **Figure 5** that the approximation (28) is a good one. $H_1(x)$ and $H_1^{approx}(x)$ seem to coincide because the difference between them is of order of 10^{-4} and hence relatively small (see **Figure 5**).

By inserting expressions (28) and (12) in the definite integral

$$I_{kn} \equiv \left\langle \psi_k^{(0)} \middle| H_1 \middle| \psi_n^{(0)} \right\rangle = \int_{-\infty}^{+\infty} \psi_k^{(0)}(x) H_1(x) \psi_n^{(0)}(x) \mathrm{d}x, \tag{33}$$

and changing variable from x to $s = \frac{1}{2}\left(1 - \tanh(\alpha x)\right)$, we find:

$$\begin{aligned} I_{kn} \approx{}& \frac{N_k N_n V_0}{2\alpha} \sum_{p=1}^{15} \tilde{B}_p \int_0^1 4^{\beta_k/2+\beta_n/2+p} s^{\beta_k/2+\beta_n/2+p-1} \\ &\times (1-s)^{\beta_k/2+\beta_n/2+p-1} {}_2F_1(-k, a_k; c_k; s)\, {}_2F_1(-n, a_n; c_n; s)\mathrm{d}s \end{aligned} \tag{34}$$

or

$$I_{kn} \approx \frac{N_k N_n}{2\alpha} V_0 \sum_{p=1}^{15} \sum_{q=0}^{k} \tilde{B}_p D(k,q) \int_0^1 4^{\beta_k/2+\beta_n/2+p} s^{\beta_k/2+\beta_n/2+p+q-1} \times (1-s)^{\beta_k/2+\beta_n/2+p-1} {}_2F_1(-n, a_n; c_n; s)\mathrm{d}s \tag{35}$$

where

$$D(k,q) = \frac{(-k)_q (a_k)_q}{(c_k)_q \, q!} \tag{36}$$

and where we have used the formula

$${}_2F_1(-k, a_k; c_k; s) = \sum_{q=0}^{k} \frac{(-k)_q (a_k)_q}{(c_k)_q \, q!} s^q. \tag{37}$$

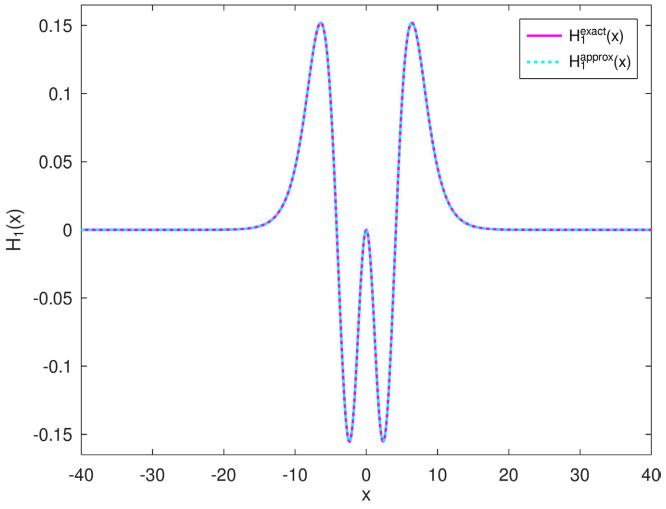

Figure 4. Variation of $H_1(x)$ given by Equation (6) and that of its approximation $H_1^{approx}(x)$.

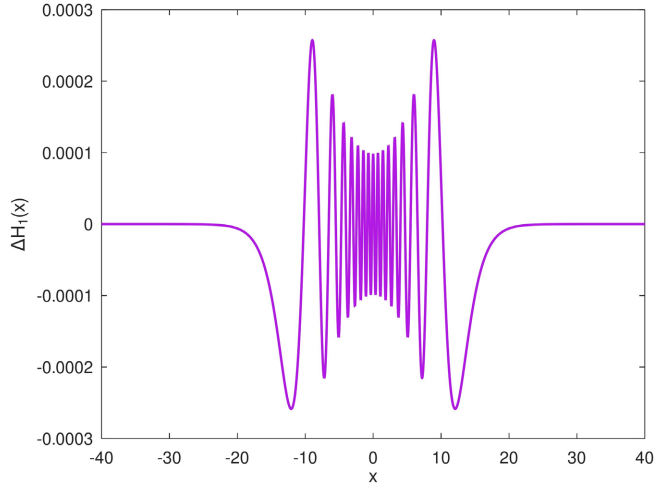

Figure 5. Error in the appriximmation of $H_1(x)$, i.e. $\Delta H_1(x) = H_1(x) - H_1^{approx}(x)$.

Using the formula [17]

$$\int_0^1 x^{\rho-1}(1-x)^{\sigma-1}\,{}_2F_1(\alpha,\beta;\gamma;x)\,\mathrm{d}x = \frac{\Gamma(\rho)\Gamma(\sigma)}{\Gamma(\rho+\sigma)}\,{}_3F_2(\alpha,\beta,\rho;\gamma,\rho+\sigma;1) \tag{38}$$

with $\Re(\rho)>0$, $\Re(\sigma)>0$ and $\Re(\gamma+\sigma-\alpha-\beta)>0$, we get

$$I_{kn} \approx \frac{N_k N_n}{2\alpha} V_0 \sum_{p=1}^{15}\sum_{q=0}^{k} \tilde{B}_p D(k,q) \frac{\Gamma(\beta_k/2+\beta_n/2+p+q)\Gamma(\beta_k/2+\beta_n/2+p)}{\Gamma(\beta_k+\beta_n+2p+q)} \times {}_3F_2(-n,a_n,\beta_k/2+\beta_n/2+p+q;c_n;\beta_k+\beta_n+2p+q;1) \tag{39}$$

3. Results and Discussion

In this section, we display our calculated results for bound state energy spectra and wave functions of the GPW for two special cases. We also compare the present approximated analytical results with the numerical ones obtained with the aid of the exact Hamiltonian diagonalization on the finite-real basis $\{\phi_n(x)\}_{n=1}^{N}$ where

$$\phi_n(x) = \sqrt{\frac{\alpha_p}{n(n+1)}} P_n^1\left(\tanh(\alpha_p)\right) \tag{40}$$

with $N=500$ and $\alpha_p = 0.01$.

Table 1 and Table 2 display bound state energies for $(V_0,\sigma)=(4.5\text{ a.u.}, 2.65\text{ a.u.})$ and $(V_0,\sigma)=\left(0.63\text{ a.u.}, 2.65/\sqrt{2}\text{ a.u.}\right)$ respectively. The unperturbed energies $E_n^{(0)}$ are reported in the second column; those containing the first- and second-order corrections are given in the third and fourth columns respectively. The numerically calculated energies E_n^{diag} are reported in the fifth column. The sixth column of Table 2 contains bound state energies found in the literature [13] for the case in question.

Table 1. Bound state energies for the GPW when $V_0 = 4.5$ a.u. and $\sigma = 2.65$ a.u.

n	$E_n^{(0)}$	E_n^{0-1}	E_n^{0-2}	E_n^{diag}
0	−4.07908569	−4.11227291	−4.11310904	−4.11314578
1	−3.28069056	−3.36615408	−3.36728309	−3.36731836
2	−2.56916237	−2.67868115	−2.67857501	−2.67869614
3	−1.94450111	−2.05060646	−2.05014342	−2.05052361
4	−1.40670681	−1.48478317	−1.48667821	−1.48693546
5	−0.95577944	−0.98735695	−0.99342876	−0.99344742
6	−0.59171902	−0.56926702	−0.57426308	−0.57792785
7	−0.31452553	−0.24748341	−0.24344728	−0.25289171
8	−0.12419899	−0.04375458	−0.03613349	−0.04298442
9	−0.02073939			

Table 2. Bound state energies for the GPW when $V_0 = 0.63$ a.u. and $\sigma = 2.65/\sqrt{2}$ a.u.

n	$E_n^{(0)}$	E_n^{0-1}	E_n^{0-2}	E_n^{diag}	$E_n^{[13]}$
0	−0.43549936	−0.44503798	−0.44503987	−0.44508672	−0.4451
1	−0.13336503	−0.13945174	−0.13945174	−0.14003911	−0.1400
2	−0.00496458	0.00176421	0.00176611	−0.00013920	-1.39×10^{-4}

The two tables show good consistency between E_n^{0-1} and E_n^{0-2} in one hand and E_n^{diag} in the other one for almost all the bound states. For energies near 0 a.u., one can notice significant differences between our results and the numerically calculated ones, which means that our method is not appropriate for highly excited bound states. Moreover, it is remarkable from Table 2 that the numerical results are better than ours. But, despite this, our method must not be neglected because it allows to obtain easily good energies and wave functions for the ground state and the first excited states.

In Figures 6-8, we show the bound state wave functions plotted against x for the two methods mentioned above. As expected, the wave functions $\psi_n^{0-1}(x)$ obtained by our method are in close agreement with those associated with the other method for the majority of bound states (those that are not highly excited).

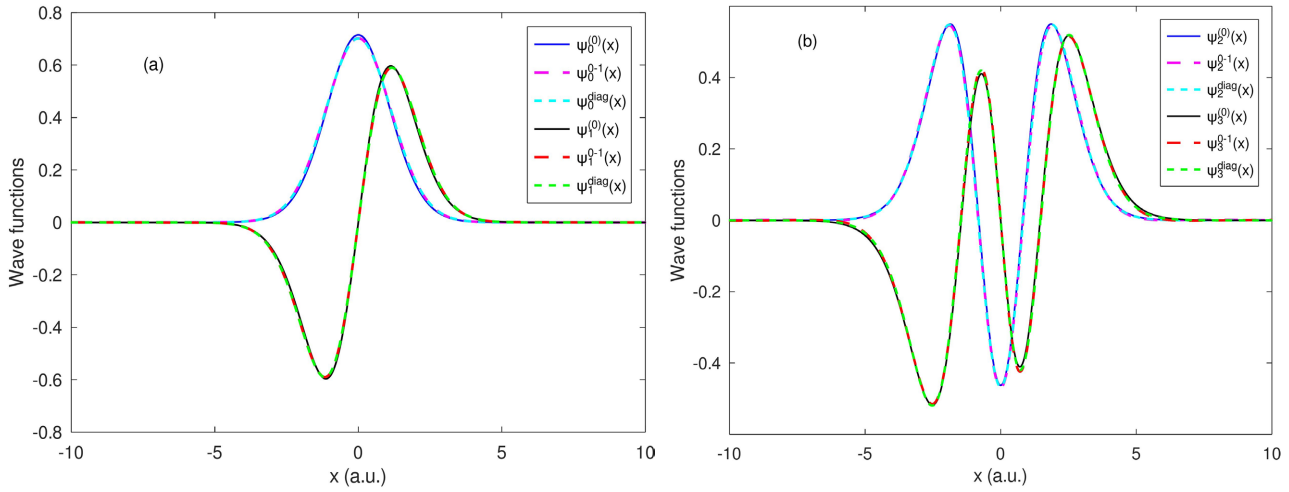

Figure 6. Wave functions for the four first bound states when $V_0 = 4.5$ a.u. and $\sigma = 2.65$ a.u. (a) $\psi_0(x)$ and $\psi_1(x)$; (b) $\psi_2(x)$ and $\psi_3(x)$.

4. Conclusions

The object of this paper has been to establish approximate analytical expressions of bound state energies and wave functions for the one-dimensional SE with the GPW. To achieve this goal, we have introduced an approximation scheme to the GPW based on the use of the MPTP and then applied the TIPT to the exact analytical solutions (eigenvalues and eigenfunctions) associated with the SE for the

MPTP. The comparison of our approximated analytical results with those obtained numerically by means of the exact Hamiltonian diagonalization led us to the following conclusions:

- Our approximation scheme to the GPW yields fairly good energies and wave functions for the majority of bound states (those that are not highly excited).
- The first- and second-order corrections, *i.e.*, $E_n^{(1)}$ and $E_n^{(2)}$, provide significant improvement in the accuracy of the energy for almost all the bound states.
- For the last bound state or the last two bound states, E_n^{0-1} can be better than E_n^{0-2}, and $\psi_n^0(x)$ can be better than $\psi_n^{0-1}(x)$ where the notation E_n^{0-j} (resp. $\psi_n^{0-j}(x)$) refers to the nth energy (resp. wave function) calculated to the jth-order (resp. the (j + 1) th-order) of perturbation theory.

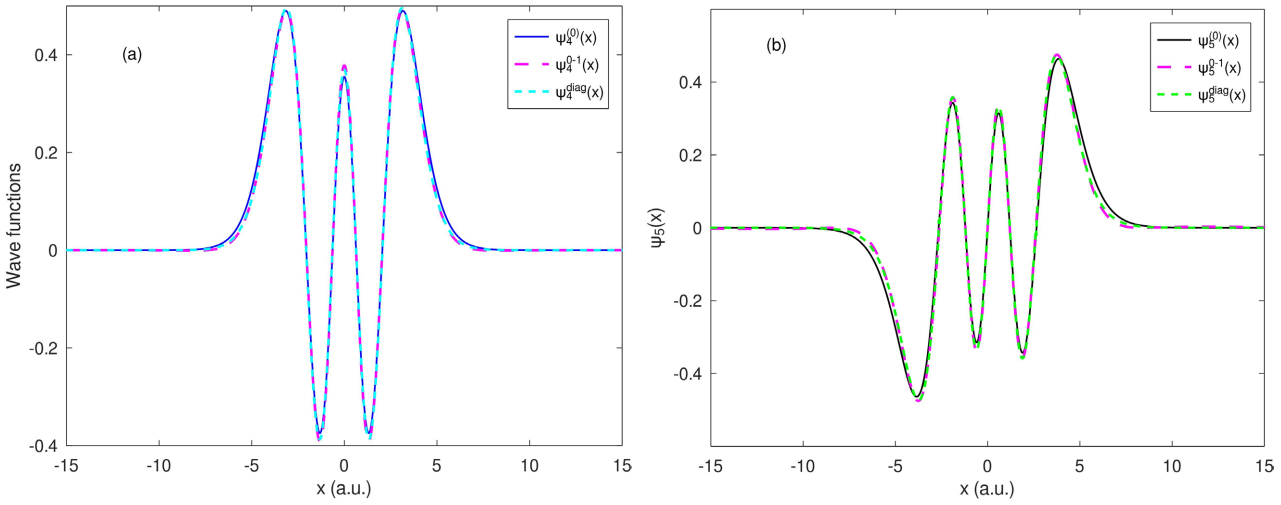

Figure 7. Wave functions for the fifth and sixth bound states when $V_0 = 4.5$ a.u. and $\sigma = 2.65$ a.u. (a) $\psi_4(x)$; (b) $\psi_5(x)$.

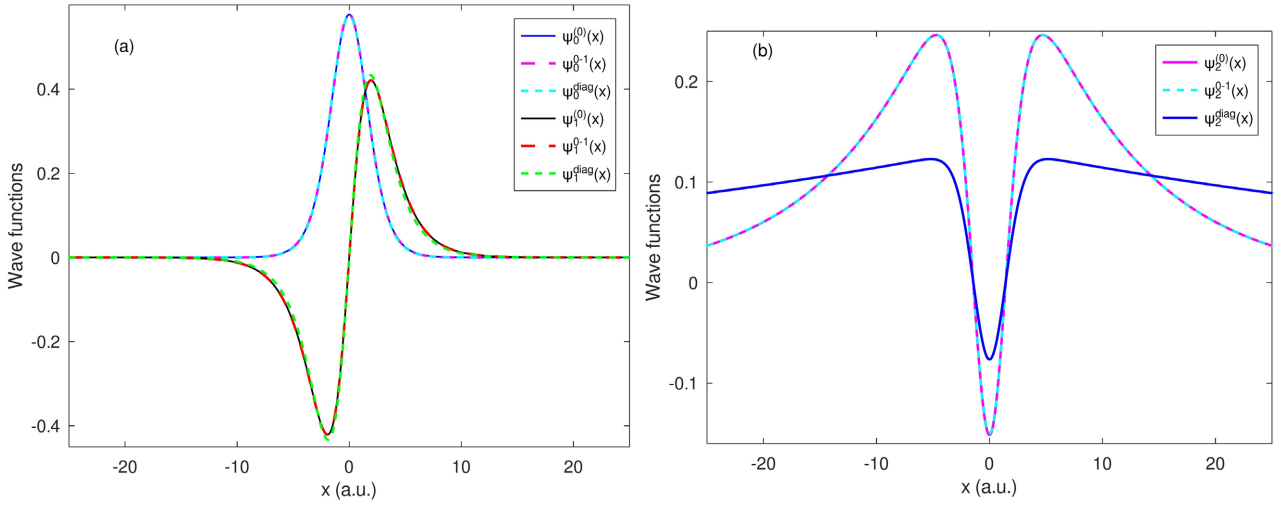

Figure 8. Bound state wave functions plotted against x for $\sigma = 2.65/\sqrt{2}$ a.u. and $V_0 = 0.63$ a.u. (a) $\psi_0(x)$ and $\psi_1(x)$; (b) $\psi_2(x)$.

Conflicts of Interest

The authors declare no conflicts of interest.

References

[1] Flügge, S. (1971) Practical Quantum Mechanics Springer-Verlag. https://doi.org/10.1007/978-3-642-61995-3

[2] Lamb, G.L. (1980) Elements of Soliton Theory. Jr. Editeur.

[3] Morse, P.M. and Feshbach, H. (1953) Methods of Theoretical Physics. MacGraw-Hill.

[4] Nieto, M.M. (1978) Exact Wave-Function Normalization Constants for the $B_0\tanh z$-$U_0\cosh^{-2}z$ and Pöschl-Teller Potentials. *Physical Review A*, **17**, 1273-1283. https://doi.org/10.1103/physreva.17.1273

[5] Nyengeri, H., Simbizi, R., Girukwishaka, A., Nizigiyimana, R. and Ndenzako, E. (2018) Frobenius Series Solutions of the Schrodinger Equation with Various Types of Symmetric Hyperbolic Potentials in One Dimension. *Open Access Library Journal*, **5**, 1-14. https://doi.org/10.4236/oalib.1104728

[6] Stephenson, G. (1977) Eigenvalues of the Schrodinger Equation with a Gaussian Potential. *Journal of Physics A*: *Mathematical and General*, **10**, L229-L232. https://doi.org/10.1088/0305-4470/10/12/003

[7] Nandi, S. (2010) The Quantum Gaussian Well. *American Journal of Physics*, **78**, 1341-1345. https://doi.org/10.1119/1.3474665

[8] Mutuk, H. (2019) Asymptotic Iteration and Variational Methods for Gaussian Potential. *Pramana*, **92**, Article No. 66. https://doi.org/10.1007/s12043-019-1729-z

[9] Mahmoud, F., Ayhan, S. and Sameer, M.I. (2022) Approximate Energy Spectra of the Quantum Gaussian Well: Four-Parameter Potential Fitting. *Jordan Journal of Physics*, **15**, 487-497. https://doi.org/10.47011/15.5.6

[10] Chen, C., Lu, F. and You, Y. (2012) Scattering States of Modified Pöschl-Teller Potential in *d*-Dimension. *Chinese Physics B*, **21**, Article ID: 030302. https://doi.org/10.1088/1674-1056/21/3/030302

[11] Nyengeri, H., Nizigiyima, R., Ndenzako, E., Bigirimana, F., Niyonkuru, D. and Girukwishaka, A. (2018) Application of the Frobenius Method to the Schrödinger Equation for a Spherically Symmetric Hyperbolic Potential. *Open Access Library Journal*, **5**, 1-15. https://doi.org/10.4236/oalib.1104950

[12] Shankar, R. (1994) Principles of Quantum Mechanics. 2nd Edition, Plenum Press.

[13] Bardsley, J.N. and Comella, M.J. (1989) Ac Stark Effect for Short-Range Potentials with Intense Electromagnetic Fields. *Physical Review A*, **39**, 2252-2255. https://doi.org/10.1103/physreva.39.2252

[14] Nouredine, Z. (2009) Quantum Mechanics Concepts and Application. 2nd Edition, John Wiley & Sons. http://www.mmmut.ac.in/News_content/02110tpnews_11232020.pdf

[15] Blinder, S.M. (2012) Energies for Particle in a Gaussian Potential Well. Wolfram. https://www.wolframcloud.com/obj/5f111c05-7eee-42b3-bf61-def6b000dff1?src=CloudBasicCopiedContent

[16] Masabarengengwa, D. (2013) Etude des Fonctions d'onde et des énergies du modèle atomique de Pöschl-Teller. Bachelor Thesis, University of Burundi.

[17] Gradshteyn, I.S. and Ryzhik, I.M. (2007) Table of Integrals, Series and Products. Academic Press.